ACS Catalysis

RESEARCH ARTICLE

pubs.acs.org/acscatalysis

Synthesis, Characterization, and Ethylene Polymerization Behavior of 8-(Nitroarylamino)-5,6,7-trihydroquinolylnickel Dichlorides: Influence of the Nitro Group and Impurities on Catalytic Activity

Liping Zhang,[†] Xiang Hao,[†] Wen-Hua Sun,*[,†] and Carl Redshaw*[,‡]

[†]Key Laboratory of Engineering Plastics, Beijing National Laboratory for Molecular Sciences, Institute of Chemistry, Chinese Academy of Sciences, Beijing 100190, China

[‡]School of Chemistry, University of East Anglia, Norwich, NR4 7TJ, U.K.

Supporting Information

ABSTRACT: The series of *N*-(5,6,7-trihydroquinolin-8-ylidene)nitroarylamine ligands (**L1**−**L4**) was prepared and used to synthesize the chloro-bridged dinickel complexes (**Ni1**−**Ni4**) and the bis-ligated mononickel(II) complex (**Ni5**) in good yield. Molecular structures of **Ni1**, **Ni2**, **Ni4**, and **Ni5** were confirmed by single-crystal X-ray diffraction analysis, revealing a pseudosquare−pyramidal geometry around nickel in the chloro-bridged complexes (**Ni1**, **Ni2**, and **Ni4**) and a distorted octahedral geometry at the nickel atom in the bis-ligated complex (**Ni5**). Upon treatment with ethylaluminum sesquichloride (EASC, $Et_3Al_2Cl_3$) or methylaluminoxane (MAO), all nickel complexes exhibited high activities (up to 4.05×10^6 g (PE) mol^{-1} h^{-1}) for ethylene polymerization. Moreover, heterocyclic impurities such as tetrahydrofuran (THF) and pyridine, often detected in common solvents, were added to the catalytic system of precatalyst **Ni2** under controlled conditions and were found to have a negative influence on the catalytic behavior during ethylene polymerization.

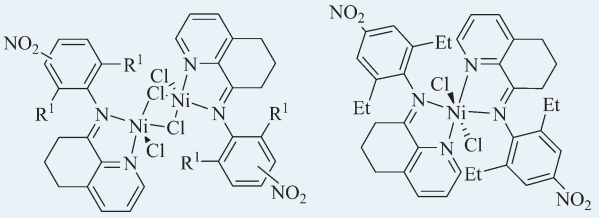

KEYWORDS: ethylene polymerization, nickel precatalyst, 2-nitroarylimino-5,6,7-trihydroquinoline, branching polyethylene, X-ray diffraction

INTRODUCTION

Since the discovery that diiminonickel dichlorides can act as highly active precatalysts in ethylene polymerization by the Brookhart group in 1995,[1] the number of papers dealing with nickel complexes as precatalysts in ethylene reactivity has mushroomed,[2−4] with the majority of these studies exploring various bidentate ligands, primarily chelating as N^N,[5−12] N^P,[13−17] N^O,[18−20] and P^O type ligand sets,[21−25] or tridentate ligands chelating as N^N^N,[26−33] N^N^O,[34] and N^P^N ligand sets.[35,36] In general, 2-iminopyridylnickel type precatalysts have drawn more attention because of their interesting catalytic behavior toward ethylene.[37−39] The 5,6,7-trihydroquinolin-8-one derivatives with fused-cycloalkanonylpyridines instead of 2-iminopyridines were recently explored, thereby forming a new series of bidentate nickel complexes, which showed high activities with unique characteristics of ethylene oligomerization by nickel precatalysts bearing 2-phenyl- or 2-chloro-substituted 8-arylamino-5,6,7-trihydroquinolines[40] and ethylene polymerization by nickel precatalysts bearing 2-substituent-free 8-arylamino-5,6,7-trihydroquinolines.[41] These results contrasted with the previous observations that bulky ligands could enhance the ethylene polymerization of late-transition metal precatalysts.[31,32,40,42−44] Different substituents can cause significant variations of the catalytic behavior performed by their metal complexes, and this is an attractive feature for complexes to be used in catalysis. Inspired by the positive influence of electron-withdrawing substituents on the catalytic performance of late-transition precatalysts,[45−48] further modification of the 8-arylamino-5,6,7-trihydroquinolines can be made by employing anilines that contain the electron-withdrawing nitro substituent (−NO_2). The newly prepared nickel complexes bearing 8-(nitroarylamino)-5,6,7-trihydroquinolines exhibited high activities in ethylene polymerization. Given that under industrial conditions, impurities are often present in the bulk solvent (toluene), the catalytic performance of a representative precatalyst herein was also evaluated in the presence of trace amounts of the heterocyclic compounds tetrahydrofuran (THF) or pyridine.

EXPERIMENTAL SECTION

General Considerations. All manipulations of air- and moisture-sensitive compounds were carried out under a nitrogen atmosphere using standard Schlenk techniques. Toluene was refluxed over sodium benzophenone and distilled under nitrogen prior to use. Methylaluminoxane (MAO, 1.46 M solution in toluene) and modified methylaluminoxane (MMAO, 1.93 M in heptane, 3A) were purchased from Akzo Nobel Corp.

Received: June 13, 2011
Revised: July 6, 2011
Published: July 18, 2011

dx.doi.org/10.1021/cs200308b | ACS Catal. 2011, 1, 1213−1220

Scheme 1. Synthetic Procedure of Nickel Complexes

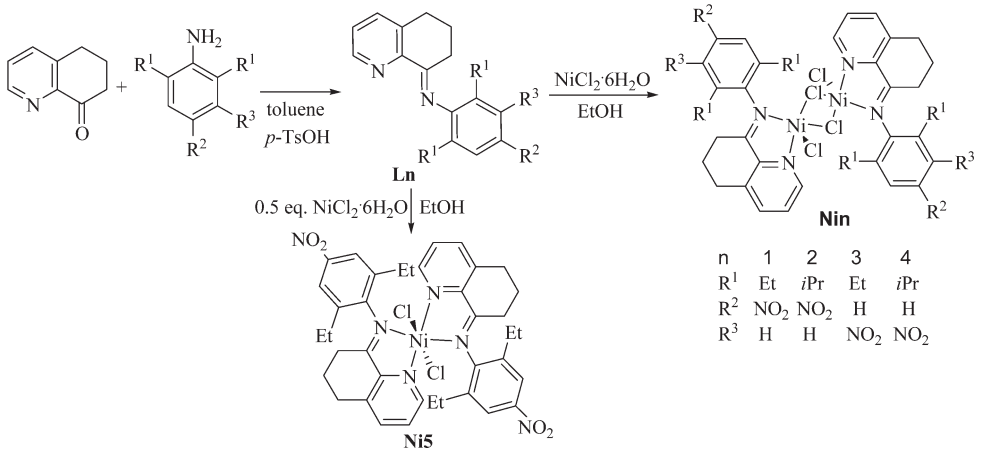

Diethylaluminum chloride (Et_2AlCl, 0.79 M in toluene) and ethylaluminum sesquinochroride (EASC, 0.87 M in toluene) was purchased from Acros Chemicals. High-purity ethylene was obtained from Beijing Yansan Petrochemical Co., and 5,6,7-trihydroquinolin-8-one was available from Astatech Inc. (www.astatechinc.com). NMR spectra were recorded on a Bruker DMX 400 MHz instrument at ambient temperature using TMS as an internal standard. IR spectra were recorded on a Perkin-Elmer system 2000 FT-IR spectrometer. Elemental analysis was carried out using a Flash EA 1112 microanalyzer. Molecular weights (M_w) and molecular weight distribution (MWD) of polyethylenes were determined by a PL-GPC220 at 150 °C with 1,2,4-trichlorobenzene as the solvent. DSC trace and melting points of polyethylene were obtained from the second scanning run on a Perkin-Elmer DSC-7 at a heating rate of 10 °C/min.

Synthesis and Characterization. Employing established synthetic procedures,[40,41] the condensation reaction of 5,6,7-trihydroquinolin-8-one with various nitroanilines in toluene provided the corresponding 8-(nitroarylamino)-5,6,7-trihydroquinolines (**L1**−**L4**), which were further reacted with an equivalent of $NiCl_2 \cdot 6H_2O$ in ethanol to form a series of nickel dichloride dimers in good yield; namely, the 8-nitroarylamino-5,6,7-trihydroquinolylnickel dichlorides (**Ni1**−**Ni4**). As a representative example, the reaction of 8-(2,6-diethyl-4-nitrophenyl)imino-5,6,7-trihydroquinoline (**L1**) with 0.5 equiv of $NiCl_2 \cdot 6H_2O$ in ethanol gave a bis-ligated mononickel complex (**Ni5**). The synthetic procedure of these compounds is illustrated in Scheme 1.

8-(2,6-Diethyl-4-nitrophenyl)imino-5,6,7-trihydroquinoline (**L1**). A solution of 5,6,7-trihydroquinolin-8-one (0.45 g, 3 mmol), 2,6-diethylaniline (0.58 g, 3 mmol), and a catalytic amount of *p*-toluenesulfonic acid in toluene (50 mL) was refluxed for 24 h. The solvent was evaporated under reduced pressure, and then the mixture was purified by column chromatography on basic silica with petroleum ether/ethyl acetate (v/v) 100:1 as eluent to afford the product as a yellow powder in 46.3% (0.45 g) yield. FT-IR (KBr, cm^{-1}): 2963.4 (w), 1641.0 (s, C═N), 1581.6 (s), 1501.6 (s), 1315.9 (s), 1102.4 (m), 895.5 (m), 792.4 (w). ^{1}H NMR (400 MHz, $CDCl_3$, TMS): δ 8.72 (d, J = 3.0 Hz, 1H, Py), 7.99 (s, 2H, Ph), 7.60 (d, J = 7.8 Hz, 1H, −Py), 7.34 (m, 1H, −Py), 2.97 (t, 2H, J = 6.1 Hz, CH_2), 2.54 (m, 2H, $-CH_2$), 2.35 (m, 4H, $-CH_2$), 1.99 (m, 2H, $-CH_2$), 1.23 (t, 6H, J = 7.5 Hz, CH_3). ^{13}C NMR (100 MHz, $CDCl_3$, TMS): δ 164.9, 154.8, 149.2, 146.3, 137.8, 137.6, 132.2, 125.6, 121.4, 121.8, 31.5, 29.4, 24.3, 22.3, 13.2. Anal. Calcd for $C_{19}H_{21}N_3O_2$ (323.39): C, 70.57; H, 6.55; N, 12.99. Found: C, 70.67; H, 6.49; N, 12.80%.

8-(2,6-Diisopropyl-4-nitrophenyl)imino-5,6,7-trihydroquinoline (**L2**). Using the same procedure as for the synthesis of **L1**, **L2** was formed as a yellow powder in 50.0% yield. FT-IR (KBr, cm^{-1}): 3044.6 (w), 2962.5 (m), 1637.7 (s, C═N), 1510.7 (s), 1322.6 (s), 1189.2 (m), 900.7 (m), 793.6 (s), 739.9 (m). ^{1}H NMR (400 MHz, $CDCl_3$, TMS): δ 8.74 (d, J = 2.9 Hz, 1H, Py), 8.04 (s, 2H, Ph), 7.61 (d, J = 7.8 Hz, 1H, −Py), 7.34 (t, J = 3.8 Hz, 1H, −Py), 2.99 (t, 2H, J = 6.0 Hz, CH_2), 2.86 (m, 2H, $-CH_2$), 2.43 (t, 2H, J = 5.8 Hz, $-CH_2$), 1.99 (m, 2H, −CH), 1.19 (d, 12H, J = 6.7 Hz, CH_3). ^{13}C NMR (100 MHz, $CDCl_3$, TMS): δ 165.1, 153.2, 149.2, 149.1, 148.1, 144.6, 137.8, 137.0, 125.6, 119.4, 31.8, 29.4, 28.5, 23.3, 22.4. Anal. Calcd for $C_{21}H_{25}N_3O_2$ (351.44): C, 71.77; H, 7.17; N, 11.96. Found: C, 71.51; H, 7.25; N, 11.50%.

8-(2,6-Diethyl-3-nitrophenyl)imino-5,6,7-trihydroquinoline (**L3**). Using the same procedure as for the synthesis of **L1**, **L3** was formed as a yellow powder in 47.8% yield. FT-IR (KBr, cm^{-1}): 2967.2 (w), 1643.2 (s, C═N), 1579.4 (s), 1321.5 (s), 1194.7 (m), 1013.9 (m), 899.0 (m), 753.8 (m). ^{1}H NMR (400 MHz, $CDCl_3$, TMS): δ 8.73 (d, 1H, J = 4.2 Hz, Py), 7.60 (d, 1H, J = 7.7 Hz, Py), 7.51 (d, 1H, J = 8.4 Hz, −Py), 7.32−7.35 (m, 1H, −Ph), 7.18 (d, 1H, J = 8.4 Hz, Ph), 2.97 (t, 2H, J = 6.0 Hz, CH_2), 2.32−2.57 (m, 6H, CH_2), 1.95−2.03 (m, 2H, $-CH_2$), 1.17 (m, 3H, J = 7.5 Hz, $-CH_3$), 1.11 (t, 3H, J = 7.3 Hz, CH_3). ^{13}C NMR (400 MHz, $CDCl_3$, TMS): δ 166.1, 149.9, 149.2, 148.9, 137.6, 137.5, 136.6, 126.5, 125.9, 125.5, 119.1, 31.4, 29.4, 27.8, 24.5, 22.3, 21.5, 13.5, 13.2. Anal. Calcd for $C_{19}H_{21}N_3O_2$ (323.39): C, 70.57; H, 6.55; N, 12.99. Found: C, 70.44; H, 6.89; N, 13.02%.

8-(2,6-Diisopropyl-3-nitrophenyl)imino-5,6,7-trihydroquinoline (**L4**). Using the same procedure as for the synthesis of **L1**, **L4** was formed as a yellow powder in 64.7% yield. FT-IR (KBr, cm^{-1}): 2966.2 (w), 2931.1 (w), 1641.9 (s, C═N), 1513.4 (s), 1311.5 (s), 1193.4 (m), 1039.9 (m), 824.0 (m), 747.7 (m). ^{1}H NMR (400 MHz, $CDCl_3$, TMS): δ 8.73 (d, 1H, J = 2.6 Hz, Py), 7.59 (d, 1H, J = 7.7 Hz, Py), 7.31 (t, 1H, J = 5.9 Hz, −Py), 7.18−7.24 (m, 2H, −Ph), 3.12−3.19 (m, 1H, CH), 2.97 (t, 1H, J = 5.9 Hz, $-CH_2$), 2.71−2.75 (m, 1H, CH), 2.38−2.46 (m, 2H, $-CH_2$), 1.95−1.99 (m, 2H, $-CH_2$), 1.28 (d, 3H, J = 6.9 Hz, CH_3),

dx.doi.org/10.1021/cs200308b |*ACS Catal.* 2011, 1, 1213–1220

Table 1. Crystal Data and Structure Refinement for Ni1·CH_2Cl_2, Ni2, Ni4 and Ni5·$2CH_2Cl_2$

	Ni1·CH_2Cl_2	Ni2	Ni4	Ni5·$2CH_2Cl_2$
empirical formula	$C_{20}H_{23}Cl_4N_3NiO_2$	$C_{21}H_{25}Cl_2N_3NiO_2$	$C_{21}H_{25}Cl_2N_3NiO_2$	$C_{40}H_{46}Cl_6N_6NiO_4$
formula weight	537.90	481.05	481.05	946.24
temperature (K)	173(2) K	173(2) K	173(2) K	173(2) K
wavelength (Å)	0.71073	0.71073	0.71073	0.71073
crystal system	triclinic	monoclinic	triclinic	triclinic
space group	*P*1	*P*2(1)/*n*	*P*1	*P*1
a (Å)	7.7306(15)	9.1206(18)	8.4918(17)	9.1269(18)
b (Å)	10.879(2)	28.489(6)	11.126(2)	10.212(2)
c (Å)	13.935(3)	9.4194(19)	14.794(3)	12.557(3)
α (°)	87.26(3)	90	107.41(3)	112.06(3)
β (°)	78.61(3)	116.45(3)	103.11(3)	96.80(3)
γ (°)	82.14(3)	90	96.34(3)	98.40(3)
V (Å^3)	1137.8(4)	2191.4(8)	1274.9(4)	1053.7(4)
Z, *D* calcd. (g·cm^{-3})	2, 1.570	4, 1.458	2, 1.253	1, 1.491
μ (mm^{-1})	1.345	1.151	0.989	0.890
F (000)	552	1000	500	490
crystal size (mm)	0.47 × 0.41 × 0.35	0.25 × 0.15 × 0.13	0.21 × 0.11 × 0.10	0.20 × 0.17 × 0.15
θ range (°)	1.49−27.48	2.59−26.35	1.50−27.48	1.78−27.48
limiting indices	$-9 \le h \le 10$	$-7 \le h \le 11$	$-10 \le h \le 11$	$-11 \le h \le 11$
	$-13 \le k \le 14$	$-35 \le k \le 35$	$-14 \le k \le 14$	$-13 \le k \le 13$
	$-18 \le l \le 18$	$-11 \le l \le 11$	$-19 \le l \le 19$	$-16 \le l \le 16$
reflections collected	13 931	15 408	15 643	13 000
independent reflections	5184 (*R* (int) = 0.0381)	4407 (*R* (int) = 0.0529)	5793 (*R* (int) = 0.0386)	4801 (*R* (int) = 0.0491)
no. of parameters	271	272	262	259
completeness to *θ* (%)	99.6%	98.5%	99.2%	99.4%
goodness of fit on F^2	1.229	1.168	1.064	1.300
final *R* indices ($I > 2\sigma(I)$)	R_1 = 0.0443 wR_2 = 0.1223	R_1 = 0.0540 wR_2 = 0.1043	R_1 = 0.0644 wR_2 = 0.1856	R_1 = 0.0643, wR_2 = 0.1590
R indices (all data)	R_1 = 0.0476 wR_2 = 0.1246	R_1 = 0.0610 wR_2 = 0.1081	R_1 = 0.0724 wR_2 = 0.1924	R_1 = 0.0753, wR_2 = 0.1703
max./min. Δ*ρ*(a) (e Å^{-3})	0.522 and −0.511	0.347 and −0.301	1.564 and −0.549	0.434 and −0.654

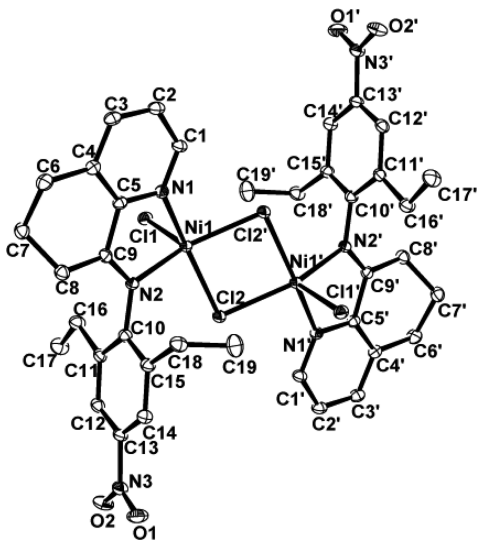

Figure 1. ORTEP drawing of **Ni1**. Thermal ellipsoids are shown at 30% probability. Hydrogen atoms and solvent molecules have been omitted for clarity.

1.14−1.18 (m, 6H, CH_3), 1.28 (d, 3H, *J* = 7.0 Hz, CH_3). ^{13}C NMR (100 MHz, $CDCl_3$, TMS): *δ* 165.1, 150.2, 149.3, 149.1, 140.2, 137.7, 137.6, 128.5, 125.4, 124.2, 122.5, 118.6, 31.6, 29.5, 28.5, 28.1, 23.8, 22.9, 22.1, 20.7, 20.2. Anal. Calcd for $C_{21}H_{25}N_3O_2$ (351.44): C, 71.77; H, 7.17; N, 11.96. Found: C, 71.84; H, 7.27; N, 11.72%.

The nickel complexes **Ni1**−**Ni4** were prepared by reacting $NiCl_2·6H_2O$ with an equivalence of the corresponding ligand in ethanol and stirring at room temperature for 12 h (Scheme 1). The precipitate was collected by filtration and washed with diethyl ether, followed by drying under vacuum. The desired complex was obtained as a light yellow powder in good yield. All complexes were isolated as air-stable powders and characterized by FT-IR spectra and elemental analyses.

Data for ***Ni1***. Yield: 78.3%. ν_{max} (KBr)/cm^{-1}: 3152.8 (w), 1519.8 (m), 1583.1 (s), 1519.8 (vs), 1461.7 (m), 1456.4 (m), 1353.8 (s), 1192.0 (m), 902.0 (m), 745.3 (m). Anal. Calcd for $C_{19}H_{21}N_3O_2NiCl_2$ (452.99): Calcd C, 50.38; H, 4.67; N, 9.28. Found: C. 50.62; H, 4.47; N, 9.72%.

Data for ***Ni2***. Yield: 85.1%. ν_{max} (KBr)/cm^{-1}: 3159.5 (w), 1622.9 (s), 1584.6 (s), 1521.7 (vs), 1456.8 (s), 1350.6 (s), 1324.6 (s), 902.4 (w), 745.1 (m). Anal. Calcd for $C_{21}H_{25}N_3O_2NiCl_2$ (481.04): Calcd C, 52.43; H, 5.24; N, 8.74. Found: C, 52.71; H, 5.35; N, 8.48%.

Data for ***Ni3***. Yield: 72.9%. ν_{max} (KBr)/cm^{-1}: 3215.5 (w), 1615.5 (m), 1581.9 (s), 1512.9 (vs), 1456.0 (m), 1337.2 (s), 1038.7 (m), 805.3 (m), 749.2 (w). Anal. Calcd for

dx.doi.org/10.1021/cs200308b |*ACS Catal.* 2011, 1, 1213–1220

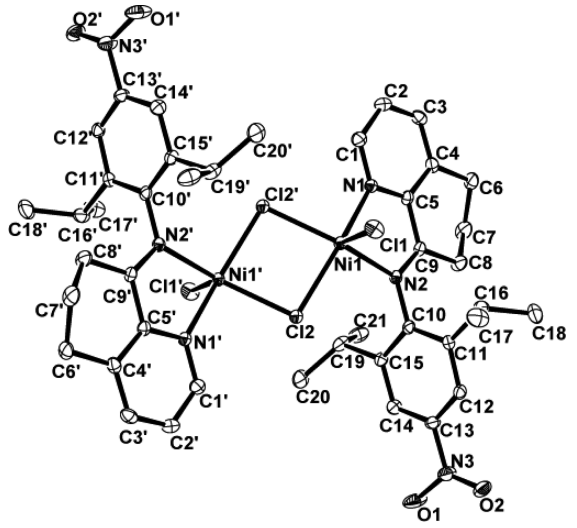

Figure 2. ORTEP drawing of **Ni2**. Thermal ellipsoids are shown at 30% probability. Hydrogen atoms and solvent molecules have been omitted for clarity.

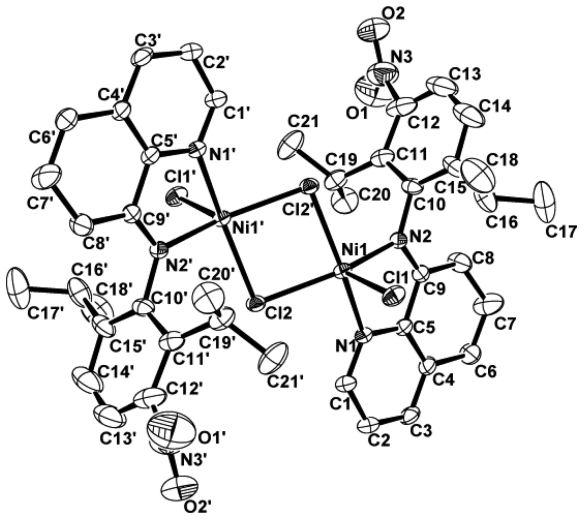

Figure 3. ORTEP drawing of **Ni4**. Thermal ellipsoids are shown at 30% probability. Hydrogen atoms and solvent molecules have been omitted for clarity.

$C_{19}H_{21}N_3O_2NiCl_2$ (452.99): Calcd C, 50.38; H, 4.67; N, 9.28. Found: C, 50.43; H, 4.33; N, 9.57%.

Data for ***Ni4***. Yield: 81.4%. ν_{max} (KBr)/cm^{-1}: 3226.2 (w), 1620.3 (m), 1584.7 (s), 1516.6 (vs), 1457.2 (m), 1356.5 (s), 1215.6 (m), 1045.5 (m), 757.6 (m). Anal. Calcd for $C_{21}H_{25}N_3O_2NiCl_2$ (481.04): Calcd C, 52.43; H, 5.24; N, 8.74. Found: C, 52.48; H, 5.11; N, 8.63%.

Data for ***Ni5***. Yield: 66.8%. ν_{max} (KBr)/cm^{-1}: 2962.7 (w), 1625.0 (m), 1581.2 (s), 1516.3 (vs), 1458.3 (m), 1323.9 (s), 1113.8 (m), 902.0 (m), 742.6 (m). Anal. Calcd for $C_{38}H_{42}N_6O_4NiCl_2$ (776.38): Calcd C, 58.79; H, 5.45; N, 10.82. Found: C, 58.43; H, 5.83; N, 10.57%.

X-ray Crystallographic Studies. Crystals of **Ni1**·CH_2Cl_2, **Ni2**, **Ni4**, and **Ni5**·$2CH_2Cl_2$ were obtained by layering diethyl ether onto dichloromethane at room temperature. With graphite-monochromated Mo Kα radiation (λ = 0.71073 Å) at 173(2) K, cell parameters were obtained by global refinement of the positions of all collected reflections. Intensities were corrected for Lorentz and polarization effects and empirical absorption. The structures were solved by direct methods and refined by full-matrix least-squares on F^2. All hydrogen atoms were placed in calculated positions. Structure solution and refinement were performed by using the SHELXL-97 package.[49] Details of the X-ray structure determinations and refinements are provided in Table 1.

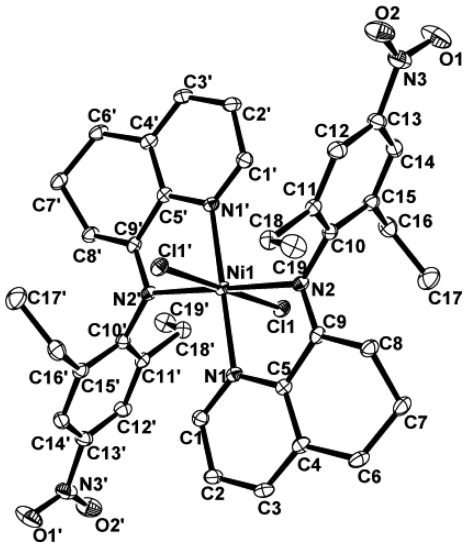

Figure 4. ORTEP drawing of **Ni5**. Thermal ellipsoids are shown at 30% probability. Hydrogen atoms and solvent molecules have been omitted for clarity.

Table 2. Selected Bond Lengths (Å) and Angles (°) for Ni1·CH_2Cl_2, Ni2, Ni4, and Ni5·$2CH_2Cl_2$

	Ni1·CH_2Cl_2	Ni2	Ni4	Ni5·$2CH_2Cl_2$
		Bond Lengths (Å)		
Ni1−N1	2.040(2)	2.035(3)	2.046(3)	2.083(3)
Ni1−N2	2.097(2)	2.085(3)	2.090(3)	2.256(3)
Ni1−Cl1	2.2887(11)	2.2565(13)	2.2794(12)	2.3601(10)
Ni1−Cl2	2.3530(9)	2.3627(10)	2.3705(12)	
N1−C1	1.331(3)	1.339(4)	1.334(5)	1.337(4)
N2−C9	1.290(3)	1.290(4)	1.278(5)	1.283(4)
N2−C10	1.436(3)	1.432(4)	1.450(5)	1.439(4)
		Bond Angles (°)		
N1−Ni1−N2	78.84(9)	79.17(10)	78.82(12)	76.35(11)
N1−Ni1−Cl1	94.18(7)	97.40(8)	92.42(10)	87.30(8)
N1−Ni1−Cl2	163.92(7)	161.30(8)	93.63(9)	
N2−Ni1−Cl1	103.47(7)	103.20(8)	101.82(9)	90.99(8)
N2−Ni1−Cl2	93.57(7)	94.29(7)	152.50(9)	
Cl1−Ni1−Cl2	101.42(4)	101.16(4)	104.92(5)	

Procedure for Ethylene Polymerization. Ethylene polymerization at 10 atm ethylene pressure was carried out in a 250 mL stainless steel autoclave equipped with a mechanical stirrer and a temperature controller. Toluene, the desired amount of cocatalyst, and a toluene solution of the catalytic precursor (the total volume was 100 mL) were added to the reactor in this order

dx.doi.org/10.1021/cs200308b |*ACS Catal.* 2011, 1, 1213–1220

Table 3. Selection of Suitable Alkylaluminum by Precatalyst Ni2[a]

entry	cat.	cocat.	Al/Ni	T (°C)	PE (g)	activity[b]	T_m[c] (°C)	M_w[d] (kg mol^{-1})	M_w/M_n[d]
1	**Ni2**	MMAO	1000	20	4.40	1.76	84.3		
2	**Ni2**	MAO	1000	20	7.81	3.12	116.6	3.9	2.6
3	**Ni2**	Et_2AlCl	200	20	2.61	1.05	76.8		
4	**Ni2**	EASC	200	20	5.91	2.36	114.5	12	6.8

[a] Reaction conditions: 5 μmol; 10 atm of ethylene; 30 min; 100 mL of toluene. [b] 10^6 g·mol^{-1} (Ni)·h^{-1}. [c] Determined by DSC. [d] Determined by GPC.

Table 4. Ethylene Polymerization with Nickel Precatalysts/EASC[a]

entry	cat.	Al/Ni	T (°C)	PE (g)	activity[b]	T_m[c] (°C)	M_w[d] (kg mol^{-1})	M_w/M_n[d]	branches/1000C
1	**Ni2**	200	20	5.91	2.36	114.5	12	6.8	116[e]
2	**Ni2**	300	20	6.47	2.59	117.4	2.9	2.6	119[e]
3	**Ni2**	400	20	10.1	4.05	113.4	1.9	1.7	101[e], 116[f]
4	**Ni2**	500	20	9.67	3.87	118.6	1.9	1.6	94[e]
5	**Ni2**	600	20	8.63	3.45	113.8	1.8	1.5	97[e]
6	**Ni2**	400	30	8.39	3.36	117.1	1.7	1.5	90[e]
7	**Ni2**	400	50	3.32	1.33	115.2	5.0	4.6	98[e]
8	**Ni1**	400	20	6.83	2.73	112.9	5.1	2.6	114[e]
9	**Ni3**	400	20	4.37	1.75	119.2	1.9	1.6	87[e]
10	**Ni4**	400	20	8.97	3.59	113.3	2.4	2.0	103[e]
11	**Ni5**	400	20	4.64	1.87	118.3	4.8	3.4	116[e]

[a] Reaction condition: 5 μmol; 30 min; 10 atm of ethylene; 100 mL of toluene. [b] 10^6 g·mol^{-1} (Ni)·h^{-1}. [c] Determined by DSC. [d] Determined by GPC. [e] Determined by FT-IR.[54] [f] Determined by ^{13}C NMR[55] (see Figure 5).

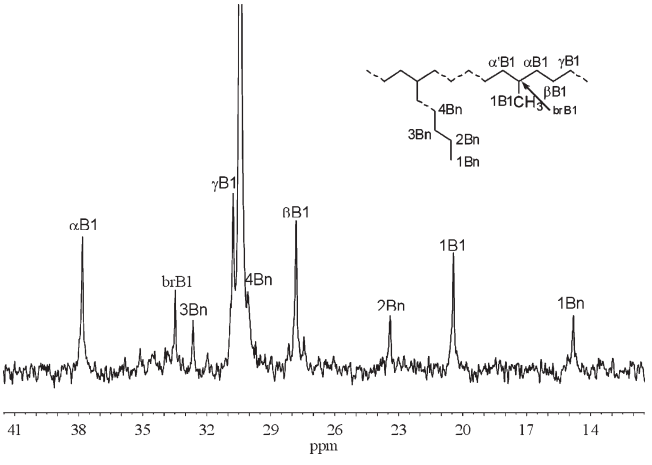

Figure 5. ^{13}C NMR spectrum of polyethylene prepared by system **Ni2**/EASC (entry 3, Table 4).

under an ethylene atmosphere. When the desired reaction temperature was reached, the ethylene pressure was increased to 10 atm and maintained at this level by constant feeding of ethylene. After the desired reaction time, the reaction was quenched by addition of acidic ethanol. The precipitated polymer was washed with ethanol and water several times and then dried in vacuum.

General Procedure for Ethylene Polymerization in the Presence of a Heterocyclic Adduct. The reactor was pressurized with 1.0 atm of ethylene, and the desired amount of cocatalyst, a toluene solution of the catalytic precursor, and 0.02 mL of the degassed heterocyclic adduct (THF or pyridine) were quickly syringed in while maintaining the total solution volume as 100 mL. The pressure was swiftly increased to 10 atm of ethylene for 30 min with rapid stirring. After the desired reaction time, the reactor was vented, and the reaction mixture was quickly quenched with 10% HCl in methanol. The precipitated polymer was stirred for several hours, filtered, and washed with methanol. It was then dried under high vacuum overnight.

RESULTS AND DISCUSSIONS

Synthesis and Characterization of Organic Compounds and Nickel Complexes. The *N*-(5,6,7-trihydroquinolin-8-ylidene)-4-nitrobenzenamines (**L1**−**L4**) were routinely synthesized by the condensation reaction of 5,6,7-trihydroquinolin-8-one with aniline derivatives according to our previous procedure.[40,41] Different from our previous work, all of these ligands are air-stable yellow powders and were formed in moderate yields. The nickel complexes (**Ni1**−**Ni4**) were prepared by reacting $NiCl_2 \cdot 6H_2O$ with an equivalent of the corresponding ligand in ethanol and stirring at room temperature for 12 h (Scheme 1). Using the same procedure, the light green powder **Ni5** was obtained by the reaction of $NiCl_2 \cdot 6H_2O$ with 2 equiv of 2,6-diethyl-*N*-(5,6,7-trihydroquinolin-8-ylidene)-4-nitrobenzenamine (**L1**). All complexes (**Ni1**−**Ni5**) were isolated as air-stable light yellow powders in high yields. Compared with the IR spectra of the free ligands, the C═N stretching vibrations in complexes **Ni1**−**Ni5** were shifted to lower frequencies in the region 1580−1585 cm^{-1}, indicating effective coordination between the imino nitrogen atom and the nickel center. The molecular structures of the complexes **Ni1**, **Ni2**, **Ni4**, and **Ni5** were further confirmed by single-crystal X-ray diffraction.

dx.doi.org/10.1021/cs200308b |ACS Catal. 2011, 1, 1213–1220

Table 5. Ethylene Polymerization with Nickel Precatalyst/MAO [a]

entry	cat.	Al/Ni	T (°C)	PE (g)	activity[b]	T_m[c] (°C)	M_w[d] (kg mol^{-1})	M_w/M_n[d]	branches/1000C
1	**Ni2**	500	20	5.23	2.09	118.9	5.4	2.6	95[e]
2	**Ni2**	750	20	6.40	2.56	117.4	4.7	2.4	89[e]
3	**Ni2**	1000	20	7.81	3.12	116.6	3.9	2.6	93[e],130[f]
4	**Ni2**	1250	20	7.69	3.08	114.7	4.4	2.6	122[e]
5	**Ni2**	1500	20	7.05	2.82	113.6	2.8	1.8	110[e]
6	**Ni2**	1000	30	3.82	1.53	119.3	3.0	2.2	98[e]
7	**Ni2**	1000	50	2.90	1.16	113.4	2.0	1.9	117[e]
8	**Ni1**	1000	20	3.88	1.55	117.1	3.5	2.0	94[e]
9	**Ni3**	1000	20	4.50	1.80	121.1	11	4.5	101[e]
10	**Ni4**	1000	20	5.28	2.11	119.9	23	7.6	116[e]
11	**Ni5**	1000	20	2.24	0.90	117.9	3.9	2.2	98[e]

[a] Reaction conditions: 5 μmol; 10 atm of ethylene; 30 min; 100 mL of toluene. [b] 10^6 g·mol^{-1} (Ni)·h^{-1}. [c] Determined by DSC. [d] Determined by GPC. [e] Determined by FT-IR.[54] [f] Determined by ^{13}C NMR [55] (see Figure 6).

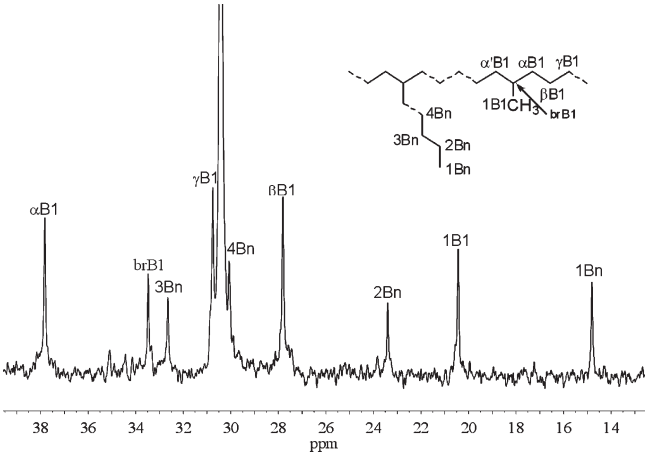

Figure 6. ^{13}C NMR spectrum of polyethylene prepared by system **Ni2**/MAO (entry 3, Table 5).

Molecular Structures. The molecular structures are shown in Figures 1−4, and their selected bond lengths and angles are collected in Table 2.

The complexes **Ni1**, **Ni2**, and **Ni4** adopt similar structures, comprising a dimer in which the two nickel centers are linked by two bridging chloride atoms. The resultant five-coordinate nickel atoms adopt pseudo-square−pyramidal geometries. As an example, consider **Ni1** (see Figure 1). The square pyramidal geometry around the nickel atoms was completed by the two bridging chlorine atoms and one chloride and bidentate ligand. There is a quadrilateral center formed with Ni1, Cl2, Ni1′ and Cl2′, but there is no direct interaction between the two nickel atoms, as evidenced by the intramolecular distance of 3.438 Å, which is slightly shorter than observed in the analogous iminopyridine−Ni(II) dimers.[50] Within the nickel-pentacyclic plane of Ni1, N1, C5, C9, and N2, the nickel atom protrudes slightly, by 0.0545 Å. Comparing of the bond lengths around the nickel center, it is seen that the Ni1−Cl1 (terminal, 2.2887(11) Å) is shorter than the Ni1−Cl2 (bridging, 2.3530(9) Å), whereas the bond length of Ni1−N2 (2.097 (2) Å) and Ni1−N1 (2.040 (2) Å) also differ slightly. The aryl ring and the chelate plane comprising N1−C5−C9−N2 are near perpendicular, with a dihedral angle of 93.3°. Similar structural parameters were observed within the complexes **Ni2** and **Ni4**, with slight differences of Ni−Cl bond lengths due to the influence of their different ligands.

Complex **Ni5** (Figure 4) possesses a distorted octahedral environment at the nickel center, comprising four N atoms of the chelate ligands and two chlorides, affording a centosymmetric structure. Due to more donating ligands, the Ni−N bond lengths are elongated in complex **Ni5** compared with its analog nickel complexes.

Ethylene Polymerization. Because of the previous good catalytic performance by the nickel precatalyst bearing *ortho*-isopropyl on the imino-bound phenyl group in our previous work,[41] precatalyst **Ni2** was typically investigated using various alkylaluminum reagents, such as MAO, MMAO, Et_2AlCl, and EASC as cocatalysts in ethylene polymerization (entries 1−4, Table 3). The highest activity was observed by employing MAO as cocatalyst (entry 2, Table 3). The less expensive cocatalyst ethylaluminum sesquichloride ($Et_3Al_2Cl_3$, EASC) (entry 4, Table 3) also activated the catalytic system with high activity. As a consequence, both the cocatalysts EASC and MAO were selected for further investigation.

Catalytic Performance in the Presence of EASC as Cocatalyst. Using EASC as cocatalyst, the optimization of the reaction parameters was conducted with precatalyst **Ni2**, and the results are tabulated in Table 4 (entries 1−7) with the optimum conditions of Al/Ni molar ratio of 400 at 20 °C (entry 3, Table 4). On increasing the molar ratio of Al/Ni from 200 to 600 (entries 1−5, Table 4), interestingly, the M_w and M_w/M_n values of the polyethylene formed showed little variation, indicating similar polyethylenes were produced. Increasing the reaction temperature (entries 3, 6, 7, Table 4) resulted in the observation of lower catalytic activities in the catalytic system, which is consistent with previous trends for the thermoinstability of the active species in common N^N-bidentate type nickel precatalysts.[51−53] Narrow M_w/M_n values were observed for the polyethylene obtained at either 20 or 30 °C (entries 3−6, Table 4), indicative of the formation of a single-site active species. The polyethylenes herein obtained had molecular weights ranging from 3.0 to 5.0 kg mol^{-1} and molecular weight distributions of between 1.4 and 4.6. The numbers of branches were calculated according to the FT-IR spectra of the obtained polyethylene according to the literature method.[54] The branch information of one representative polyethylene (entry 3, Table 4) was confirmed by ^{13}C NMR spectroscopic analysis[55]

Table 6. Ethylene Polymerization by Ni2 Affected by THF or Py[a]

entry	polar solvent	cocat.	Al/Ni	PE (g)	activity[b]	T_m[c] (°C)	M_w[d] (kg mol^{-1})	M_w/M_n[d]	branches/1000C
1	THF	EASC	400	2.78	1.11	112.5	4.5	2.9	120[e]
2	THF	MAO	1000	3.86	1.54	114.5	3.0	1.9	126[e]
3	Py	EASC	400	2.80	1.12	112.9	3.7	2.2	127[e]
4	Py	MAO	1000	3.64	1.46	116.1	2.4	1.9	103[e]

[a] Reaction condition: 5 μmol of complex **Ni2**; 20 °C; 0.2 mL of (THF or Py); 10 atm of ethylene; 100 mL of toluene. [b] 10^6 g·mol^{-1} (Ni)·h^{-1}. [c] Determined by DSC. [d] Determined by GPC. [e] Determined by FT-IR.[54]

(shown in Figure 5). The highly branched polyethylenes were caused via polymeric chain migration on the active nickel species, and such migration also resulted in enhanced bulk around the active center and termination of the polymerization reaction, thereby forming polyethylene of reduced molecular weight. The scope of applications of these highly branched polyethylenes is worthy of further exploration.

Using the optimum conditions of the Al/Ni molar ratio of 400 at 20 °C under 10 atm of ethylene, all nickel complexes were investigated (entries 3, 8−11, Table 4). With regard to the different R^1 groups at the meta position of the *N*-aryl rings, bulkier R^1 groups enhanced the catalytic activities of their nickel precatalysts. For example, **Ni2** > **Ni1** (entries 3 and 8, Table 4) and **Ni4** > **Ni3** (entries 10 and 9, Table 4). Such phenomena are consistent with observations in the literature that bulkier alkyl substituents help to solubilize the precatalysts thereby enhancing activity.[31,32,40−44]

The influence of the nitro group position was also observed by comparing the activities obtained for **Ni1** and **Ni3** as well as for **Ni2** and **Ni4**. The nitro substituent at the para position of the *N*-aryl group showed higher activity than when positioned at the meta position of the *N*-aryl group, that is, **Ni1** > **Ni3** (entries 8 and 9, Table 4) and **Ni2** > **Ni4** (entries 3 and 10, Table 4). The precatalyst **Ni5** also showed high activity in ethylene polymerization (entry 11, Table 4) but revealed a lower activity than did the analog **Ni1** (entry 8, Table 4). The proposed active species is $\mathbf{L}ClNi^{\oplus}$, formed in the catalytic system after the dissociation of one ligand (**L**) from the dominant species $\mathbf{L}_2ClNi^{\oplus}$.

Catalytic Performance in the Presence of MAO as Cocatalyst. Similarly, the precatalyst **Ni2** was evaluated for optimum conditions when using MAO as the cocatalyst (entries 1−7, Table 5). By varying the Al/Ni ratio from 500 up to 1000 (entries 1−5, Table 5), the most suitable Al/Ni ratio was observed at the ratio 1000:1 (entry 3, Table 5). Similar to the catalytic system generated in the presence of EASC, the catalytic activity decreased on elevating the reaction temperature from 20 to 50 °C (entries 3, 6−7, Table 5), which is probably due to the active species being partly unstable at higher temperatures. The trend for lifetime was observed to be the same as its analog.[41] The numbers of branches were also calculated according to the FT-IR spectra of the polyethylenes.[54] The branch value of the polyethylene (entry 3, Table 5) was confirmed by the ^{13}C NMR method[55] and is shown in Figure 6.

Using the optimum conditions of an Al/Ni ratio of 1000 at 20 °C, the nickel precatalysts were screened for ethylene polymerization in the presence of MAO (entries 3, 8−10, Table 5). In regard to the influence of the ligands used, catalytic behavior similar to that observed in the presence of EASC was exhibited, leading to the activity order **Ni2** > **Ni4** > **Ni3** > **Ni1**. It is worth mentioning that the polyethylene obtained with MAO possessed higher molecular weight (M_w) values than those obtained in the presence of EASC. More importantly, the current nickel precatalysts bearing ligands with additional nitro substituents required much less cocatalyst (MAO) compared with their analogs.[41]

The bis-ligated nickel complex **Ni5** was less interesting due to the lower activities exhibited (entry 11, Table 5) compared with the monoligated analog **Ni1** (entry 8, Table 5). As in our previous work,[40,41] the halo-bridged structures for the dinuclear nickel complexes existed only in the solid state, whereas active centers in solution, if monomeric species, would possess more coordination sites. Thus, the bis-ligated nickel precatalyst **Ni5** showed lower catalytic activities; such phenomena were consistent with previous observations of lower activities by nickel complexes bearing ligands with tetra-N donors versus nickel analogs containing bidenate ligands in vinyl polymerization of norbornene.[56]

Ethylene Polymerization Affected by Trace Amount of Common Heterocyclic Compounds. In our previous work, some results were not reproducible by the same precatalyst on changing the source of toluene, despite the toluene always being refluxed over sodium benzophenone and distilled under nitrogen prior to use. Traces of heterocyclic compounds were considered, and understanding this behavior will be very important for any further industrial application. Therefore, ethylene polymerization by the precatalyst **Ni2** (EASC/MAO) was conducted in a solution of toluene containing either tetrahydrofuran (THF) or pyridine (Py), and the results are tabulated in Table 6. In all cases, the activities were several times lower on adding THF or Py; there was a greater impact for the catalytic system employing EASC as cocatalyst than for that observed using MAO as cocatalyst. Moreover, there was no difference of catalytic activity observed on adding the same volume of an alkane such as hexane or heptane. In other words, the heterocyclic compounds participate in coordination to the metal center through the heteroatom and are a poisonous impurity for the ethylene polymerization process by these precatalysts.

CONCLUSIONS

Nickel complexes bearing *N*-(5,6,7-trihydroquinolin-8-ylidene)-nitrobenzenamines were synthesized and fully characterized. All nickel precatalysts, activated by either EASC or MAO, exhibited high activities for ethylene polymerization, producing polyethylene with narrow molecular weight distribution. For the catalytic system using MAO, the nickel precatalysts bearing ligands with a nitro substituent required a smaller amount of cocatalyst, which is an important cost-saving issue. The bis-ligated nickel precatalyst showed lower activities. Furthermore, the presence of heterocyclic compounds, such as THF and Py, caused deactivation of the nickel precatalysts in the ethylene polymerization. All polyethylenes obtained are highly branched and potentially useful.

dx.doi.org/10.1021/cs200308b |*ACS Catal.* 2011, 1, 1213–1220

■ ASSOCIATED CONTENT

Supporting Information. CIF file gives X-ray crystal structural data of nickel complexes **Ni1**·CH_2Cl_2, **Ni2**, **Ni4**, and **Ni5**·$2CH_2Cl_2$. These materials are available free of charge via the Internet at http://pubs.acs.org.

■ AUTHOR INFORMATION

Corresponding Author

*(W.H.S.) Phone: +86-10-62557955. Fax: +86-10-62618239. E-mail: whsun@iccas.ac.cn. (C.R.) Phone: +44 (0)1603 593137. Fax: +44 (0)1603 592003. E-mail: carl.redshaw@uea.ac.uk.

■ ACKNOWLEDGMENT

This work was supported by MOST 863 program No. 2009AA033601. C.R. thanks the EPSRC for an overseas travel grant (EP/H031855/1).

■ REFERENCES

(1) Johnson, L. K.; Killian, C. M.; Brookhart, M. *J. Am. Chem. Soc.* **1995**, *117*, 6414–6415.
(2) Ittel, S. D.; Johnson, L. K.; Brookhart, M. *Chem. Rev.* **2000**, *100*, 1169–1203.
(3) Gibson, V. C.; Spitzmesser, S. K. *Chem. Rev.* **2003**, *103*, 283–315.
(4) Mecking, S. *Coord. Chem. Rev.* **2000**, *203*, 325–351.
(5) Benito, J. M.; Jesús, E.; Mata, F. J.; Flores, J. C.; Gómez, R.; Gómez-Sal, P. *Organometallics* **2006**, *25*, 3876–3887.
(6) Killian, C. M.; Tempel, D. J.; Johnson, L. K.; Brookhart, M. *J. Am. Chem. Soc.* **1996**, *118*, 11664–11665.
(7) Svejda, S. A.; Brookhart, M. *Organometallics* **1999**, *18*, 65–74.
(8) Schmid, M.; Eberhardt, R.; Klinga, M.; Leskelä, M.; Rieger, B. *Organometallics* **2001**, *20*, 2321–2330.
(9) Camacho, D. H.; Guan, Z. *Macromolecules* **2005**, *38*, 2544–2546.
(10) Meinhard, D.; Reuter, P.; Rieger, B. *Organometallics* **2007**, *26*, 751–754.
(11) Liu, H.; Zhao, W.; Hao, X.; Redshaw, C.; Huang, W.; Sun, W.-H. *Organometallics* **2011**, *30*, 2418–2424.
(12) Song, S.; Xiao, T.; Liang, T.; Wang, F.; Redshaw, C.; Sun, W.-H. *Catal. Sci. Technol.* **2011**, *1*, 69–75.
(13) Speiser, F.; Braunstein, P.; Saussine, L.; Welter, R. *Inorg. Chem.* **2004**, *43*, 1649–1658.
(14) Tang, X.; Zhang, D.; Jie, S.; Sun, W.-H.; Chen, J. *J. Organomet. Chem.* **2005**, *690*, 3918–3928.
(15) Sun, W.-H.; Li, Z.; Hu, H.; Wu, B.; Yang, H.; Zhu, N.; Leng, X.; Wang, H. *New J. Chem.* **2002**, *26*, 1474–1478.
(16) Speise, F.; Braunstein, P. *Organometallics* **2004**, *23*, 2613–2624.
(17) Weng, Z.; Teo, S.; Hor, T. S. A. *Organometallics* **2006**, *25*, 4878–4882.
(18) Guan, Z.; Marshall, W. J. *Organometallics* **2002**, *21*, 3580–3586.
(19) Kermagoret, A.; Braunstein, P. *Dalton Trans* **2008**, *12*, 1564–1573.
(20) Hu, T.; Tang, L.; Li, X.; Li, Y.; Hu, N. *Organometallics* **2005**, *24*, 2628–2632.
(21) Keim, W. *Angew. Chem., Int. Ed., Engl.* **1990**, *29*, 235–244.
(22) Heinicke, J.; He, M.; Dal, A.; Klein, H.; Hetche, O.; Keim, W.; Flörke, U.; Haupt, H. *Eur. J. Inorg. Chem.* **2000**, 431–440.
(23) Heinicke, J.; Köhler, M.; Peulecke, N.; Keim, W. *J. Catal.* **2004**, *225*, 16–23.
(24) Guo, C.-Y.; Peulecke, N.; Basvani, K. R.; Kinderman, M. K.; Heinicke, J. *Macromolecules* **2010**, *43*, 1416–1424.
(25) Guo, C.-Y.; Peulecke, N.; Basvani, K. R.; Kinderman, M. K.; Heinicke, J. *J. Polym. Sci., Part A: Polym. Chem.* **2010**, *47*, 258–266.
(26) Kunrath, F. A.; De Souza, R. F.; Casagrande, O. L., Jr.; Brooks, N. R.; Young, V. G., Jr. *Organometallics* **2003**, *22*, 4739–4743.
(27) Ajellal, N.; Kuhn, M. C. A.; Boff, A. D. G.; Hörner, M.; Thomas, C. M.; Carpentier, J.-F.; Casagrande, O. L., Jr. *Organometallics* **2006**, *25*, 1213–1216.
(28) Al-Benna, S.; Sarsfield, M. J.; Thornton-Pett, M.; Ormsby, D. L.; Maddox, P. J.; Brés, P.; Bochmann, M. *J. Chem. Soc., Dalton Trans.* **2000**, *23*, 4247–4257.
(29) Ojwach, S. O.; Guzei, I. A.; Benade, L. L.; Mapolie, S. F.; Darkwa, J. *Organometallics* **2009**, *28*, 2127–2133.
(30) Zhang, M.; Zhang, S.; Hao, P.; Jie, S.; Sun, W.-H.; Li, P.; Lu, X. *Eur. J. Inorg. Chem.* **2007**, *24*, 3816–3826.
(31) Gao, R.; Zhang, M.; Liang, T.; Wang, F.; Sun, W.-H. *Organometallics* **2008**, *27*, 5641–5648.
(32) Chen, X.; Zhang, L.; Liang, T.; Hao, X.; Sun, W.-H. *C. R. Chim.* **2010**, *13*, 1450–1459.
(33) Chen, X.; Zhang, L.; Yu, J.; Hao, X.; Liu, H.; Sun, W.-H. *Inorg. Chim. Acta* **2011**, *370*, 156–163.
(34) Tang, X.; Sun, W.-H.; Gao, T.; Hou, J.; Chen, J.; Chen, W. *J. Organomet. Chem.* **2005**, *690*, 1570–1580.
(35) Hou, J.; Sun, W.-H.; Zhang, S.; Ma, H.; Deng, Y.; Lu, X. *Organometallics* **2006**, *25*, 236–244.
(36) Stapleton, R. L.; Chai, J.; Taylor, N. J.; Collins, S. *Organometallics* **2006**, *25*, 2514–2524.
(37) Laine, T. V.; Lappalainen, K.; Liimatta, J.; Aitola, E.; Lofgren, B.; Leskela, M. *Macromol. Rapid Commun.* **1999**, *20*, 487–491.
(38) Laine, T. V.; Piironen, U.; Lappalainen, K.; Klinga, M.; Aitola, E.; Leskelä, M. *J. Organomet. Chem.* **2000**, *606*, 112–124.
(39) Bahuleyan, B. K.; Lee, U.; Ha, C.; Kim, I. *Appl. Catal., A* **2008**, *351*, 36–44.
(40) Yu, J.; Hu, X.; Zeng, Y.; Zhang, L.; Ni, C.; Hao, X.; Sun, W.-H. *New J. Chem.* **2011**, *35*, 178–183.
(41) Yu, J.; Zeng, Y.; Huang, W.; Hao, X.; Sun, W.-H. *Dalton Trans.* **2011**, DOI:10.1039/C1DT10541H
(42) Sun, W.-H.; Li, Z.; Hu, H.; Wu, B.; Yang, H.; Zhu, N.; Leng, X.; Wang, H. *New J. Chem.* **2002**, *26*, 1474.
(43) Britovsek, G. J. P.; Mastroianni, S.; Solan, G. A.; Baugh, S. P. D.; Redshaw, C.; Gibson, C. V.; White, A. J. P.; Williams, D. J.; Elsegood, M. R. J. *Chem.—Eur. J.* **2000**, *6*, 2221–2231.
(44) Sun, W.-H.; Hao, P.; Zhang, S.; Shi, Q.; Zuo, W.; Tang, X.; Lu, X. *Organometallics* **2007**, *26*, 2720–2734.
(45) Zhang, T.; Guo, D.; Jie, S.; Sun, W.-H.; Li, T.; Yang, X. *J. Polym. Sci., Part A: Polym. Chem.* **2004**, *42*, 4765–4774.
(46) Guo, D.; Han, L.; Zhang, T.; Sun, W.-H.; Li, T.; Yang, X. *Macromol. Theory Simul.* **2002**, *11*, 1006–1012.
(47) Shi, Q.; Jie, S.; Zhang, S.; Yang, H.; Sun, W.-H. *Macromol. Symp.* **2007**, *260*, 74–79.
(48) Kuhn, P.; Sémeril, D.; Jeunesse, C.; Matt, D.; Neuburger, M.; Mota, A. *Chem.—Eur. J.* **2006**, *12*, 5210–5219.
(49) Sheldrick, G. M. *SHELXTL-97, Program for the Refinement of Crystal Structures*; University of Göttingen: Göttingen, Germany, 1997.
(50) Laine, T. V.; Klinga, M.; Leskelä, M. *Eur. J. Inorg. Chem.* **1999**, 959–964.
(51) Xiao, L.; Gao, R.; Zhang, M.; Li, Y.; Cao, X.; Sun, W.-H. *Organometallics* **2009**, *28*, 2225–2233.
(52) Hao, P.; Zhang, S.; Sun, W.-H.; Shi, Q.; Adewuyi, S.; Lu, X.; Li, P. *Organometallics* **2007**, *26*, 2439–2446.
(53) Chen, Y.; Hao, P.; Zuo, W.; Gao, K.; Sun, W.-H. *J. Organomet. Chem.* **2008**, *693*, 1829–1840.
(54) Galland, G. B.; de Souza, R. F.; Mauler, R. S.; Nunes, F. F. *Macromolecules* **1999**, *32*, 1620–1625.
(55) Usami, T.; Takayama, S. *Polym. J.* **1984**, *16*, 731–738.
(56) Eseola, A.; Zhang, M.; Xiang, J.-F.; Zuo, W.; Li, Y.; Woods, J.; Sun, W.-H. *Inorg. Chim. Acta* **2010**, *363*, 1970–1978.